Electronic Supplementary Material (ESI) for Journal of Materials Chemistry A.

Supplementary information

Specific capacitance of the graphene oxide-metal interfaces at different deoxygenation levels

Faramarz Hossein-Babaei[1,2]*, Mehrdad Naemidehkharghani[1], Reza Razmand[1]

[1]Electrical Engineering Department, Electronic Materials Laboratory, K. N. Toosi University of Technology, Tehran, 16317-14191, Iran

[2]Hezare Sevom Co. Ltd., 7, Niloofar Square, Tehran, 1533-874-417, Iran.

*corresponding author. Email: fhbabaei@kntu.ac.ir,

naemimerdas@gmail.com, razmand.reza@yahoo.com

1. Metals selection:

Much research has been conducted on the function of graphene oxide in the devices designed for the energy storage, optoelectronics, photonics, and sensors applications disregarding the properties of the GO/M interfaces involved, while all such devices require multiple metallic contacts to facilitate their connections to the external circuit. The goal was to show that the GO/M interfaces are, depending on the nature of M, of profoundly different properties which could control the specifications of the final products. Gold was the first metal selected for this purpose as it has been the only metal widely used in conjunction with GO, and it could facilitate comparison with the related data in literature. Platinum was the second M used because of its obvious chemical similarities to gold, and it demonstrated properties comparable with gold. Copper was tested as a low-cost alternative, but observing specific capacitances 10,000 times less than those of gold and platinum intrigued the authors to inspect the interface structure further and bring in two base metals with vast electrochemical applications, Al and Zn, for similar investigations. The introduction of Ti has been due to the model established for the GO/Cu, GO/Zn, and GO/Al placing emphasis on the oxide/hydroxide grown on the metal. It is well known that the native oxide grown on Ti is of very different dielectric properties, and it was conceived that the interface should demonstrate distinct properties. Our findings are anticipated to initiate research on the electrical properties of GO interfaces with other metals.

2. Comparison with previous reports

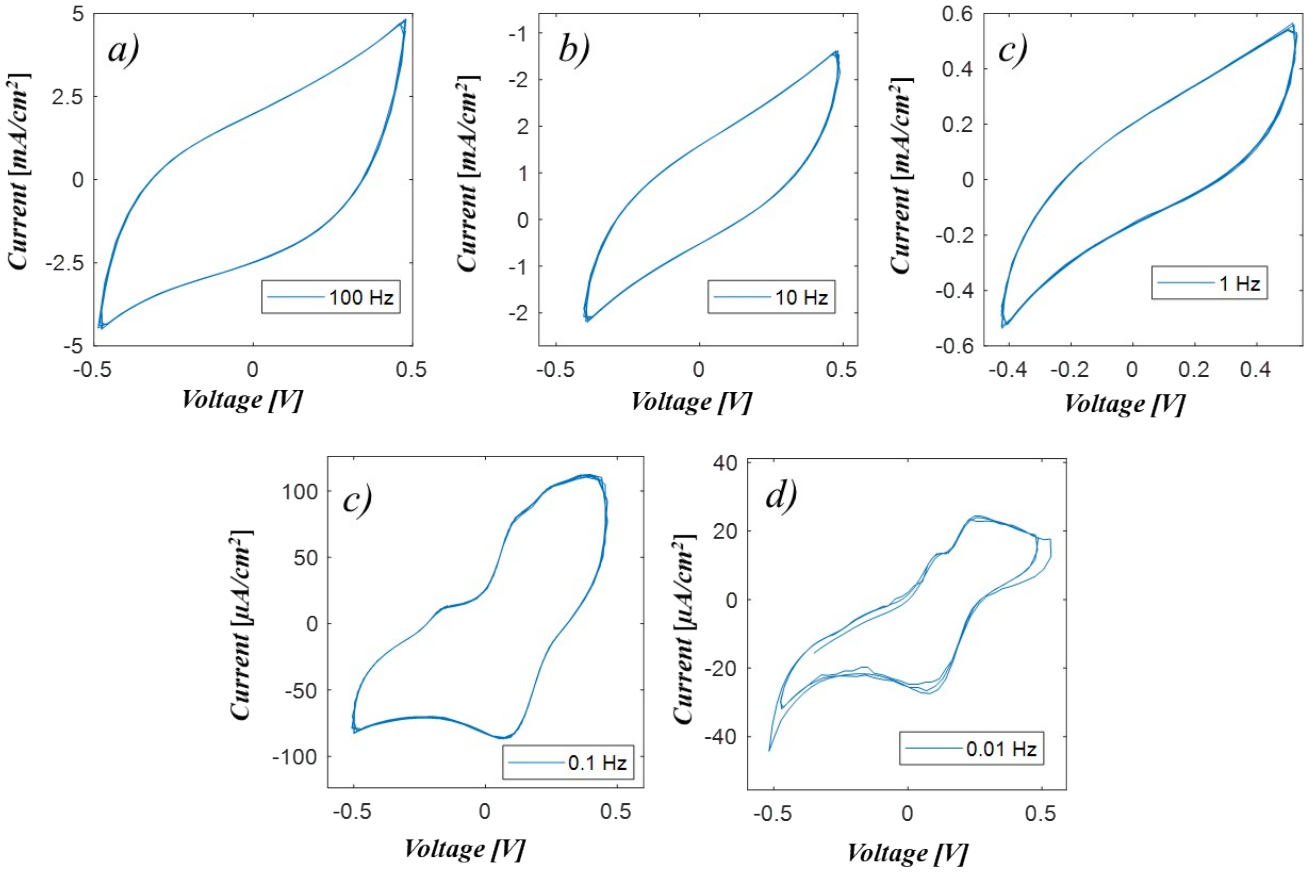

Figure S1. The I-V characteristics recorded for a GO/Au sample at the stated frequencies (**a-d**).

Table S1. A summary of the specific capacitances obtained for the GO/Au samples and their comparison with respective data available in the literature.

Sample Structure	**Current collector**	**Electrolyte**	**Capacitance**	**Reference**
Au/GO/Au Drop cast GO layer	Au	-	20 uF/cm^2 at 100 Hz, 45 uF/cm^2 at 10 Hz, 130 uF/cm^2 at 1 Hz, 540 uF/cm^2 at 0.1 Hz, 830 uF/cm^2 at 0.01 Hz	This work
RGO/GO/RGO Fiber	Au	BMIMBF4	0.4 mF/cm^2 at 0.2 V/s	[S1]
RGO/GO/RGO Paper	Au	-	1mF/cm^2 at 0.3 V/s	[S2]
RGO/GO/RGO Paper	Au	H2SO4 Intercalated GO	8.92 mF/cm^2, 0.2 V/s	[S3]
RGO/GO/RGO Paper	-	Hydrated GO	1 mF/cm^2	[S4]

3. The insensitivity to GO thickness variation:

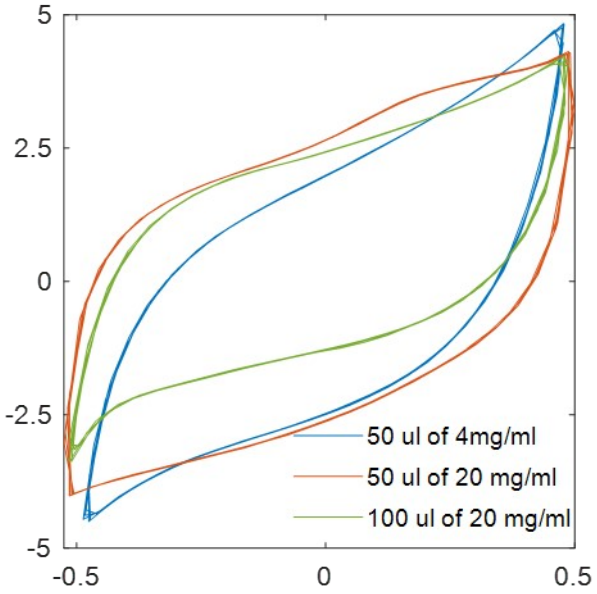

Figure S2. The I-V characteristics of analogous GO/Au samples different in GO thickness; the approximate GO thicknesses are given as legends; the frequency of the voltage waveform used for the I-V plotting is 100 Hz.

4. The experimental results related to GO/Pt samples

The investigations described in the Results Sec. of the manuscript for GO/Au are repeated on the analogous GO/Pt samples. A platinum rod is used as the current collector (**Figure S3a**). The results (**Figure S3b-c** and **Figure S4a-c**) depict similar trends of variations to those presented in **Figures 1c-d** and **2a-c** for the GO/Au samples. The recorded *SC* values are of the same order of magnitude as in GO/Au samples.

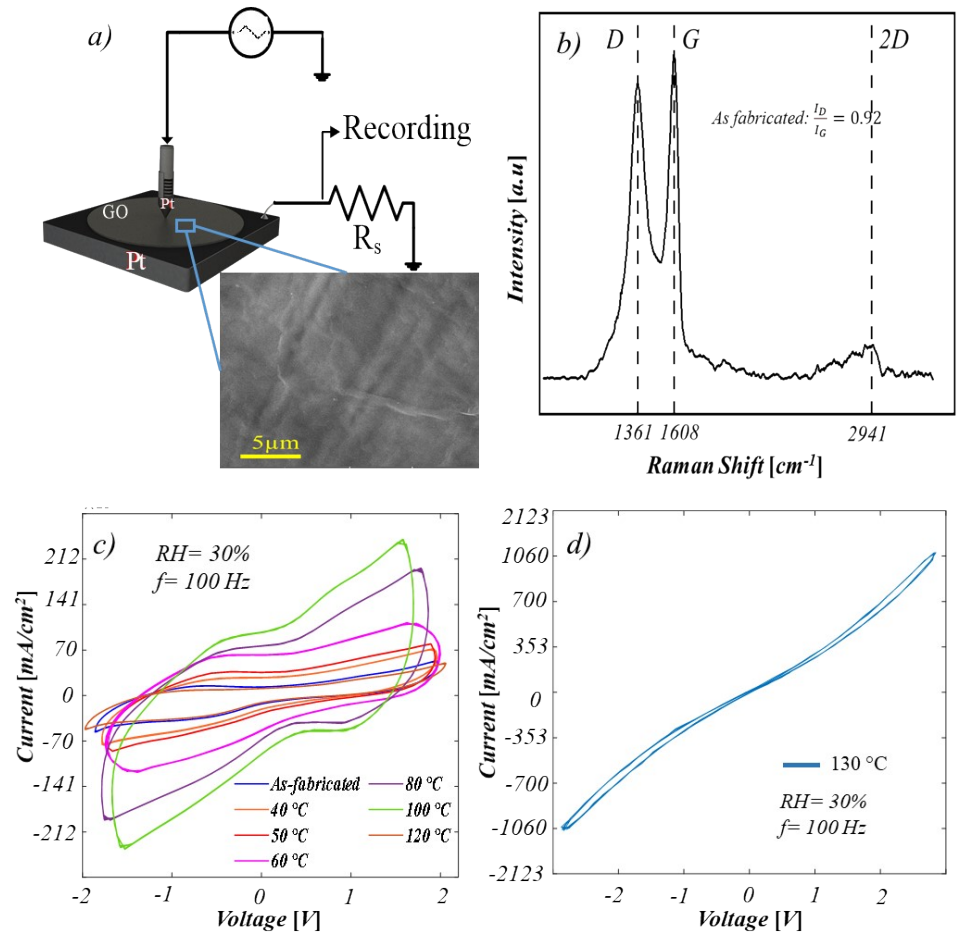

Figure S3. The characterization results on GO/Pt samples; (**a-d**) have the same significances as the respective ones in **Figure 1**.

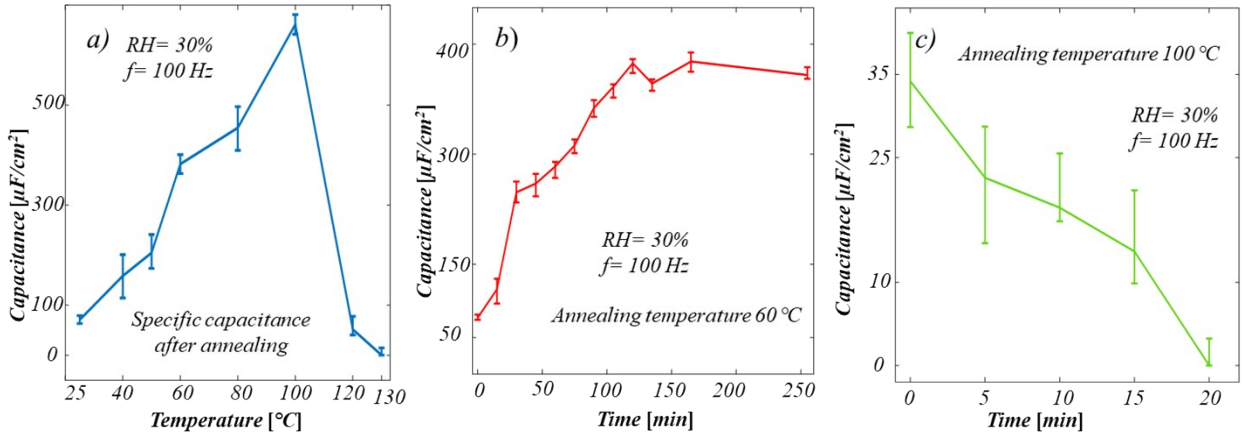

Figure S4. The irreversible variations of the *SC* of GO/Pt samples caused by thermal annealing; (**a**)-(**c**) have the same respective significances of the respective frames in **Figure 2**.

5. GO/Zn and GO/Al

Zinc and aluminum have both been used as electrodes in the electrochemical energy generation and storage devices. [S5,S6]The fabrication method and testing protocol utilized for GO/Zn and GO/Al samples are similar to those reported for the GO/Au. The results in both cases, presented respectively in **Figures S5-S6** and **Figures S7-S8**, resemble those reported for the GO/Cu samples.

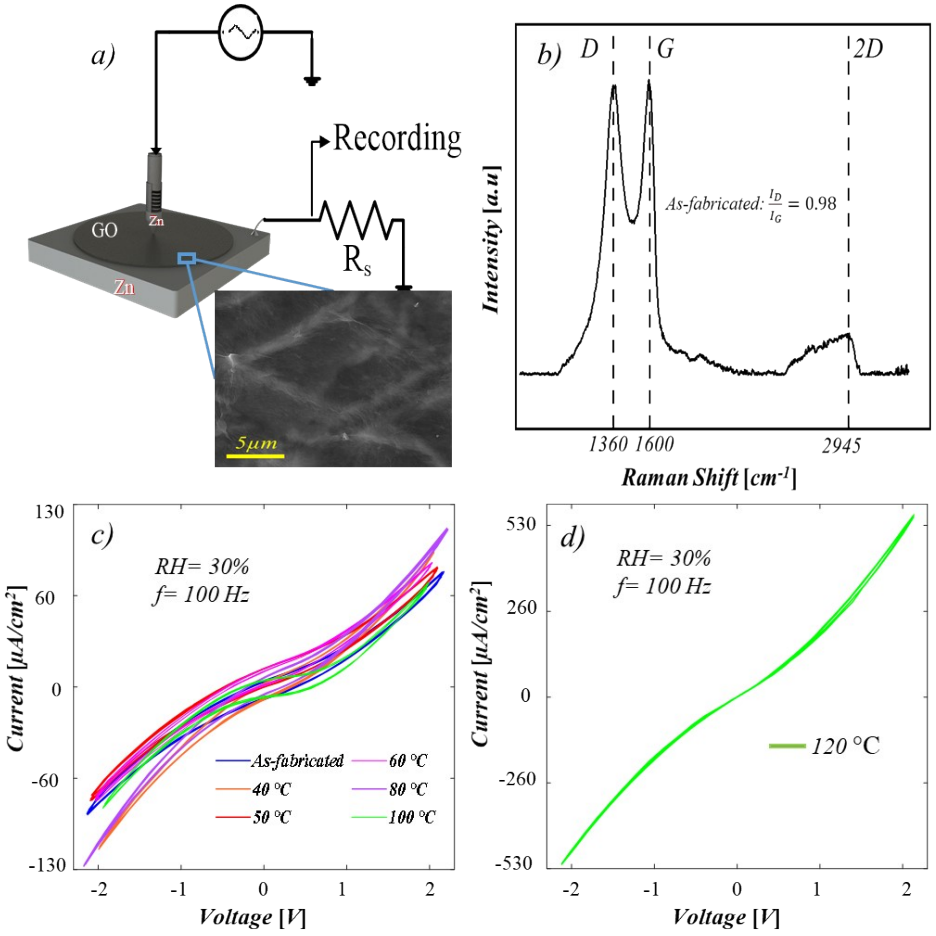

Figure S5. The characterization results on a GO/Zn sample; the presented frames have the same significances as the respective ones in **Figure 1**.

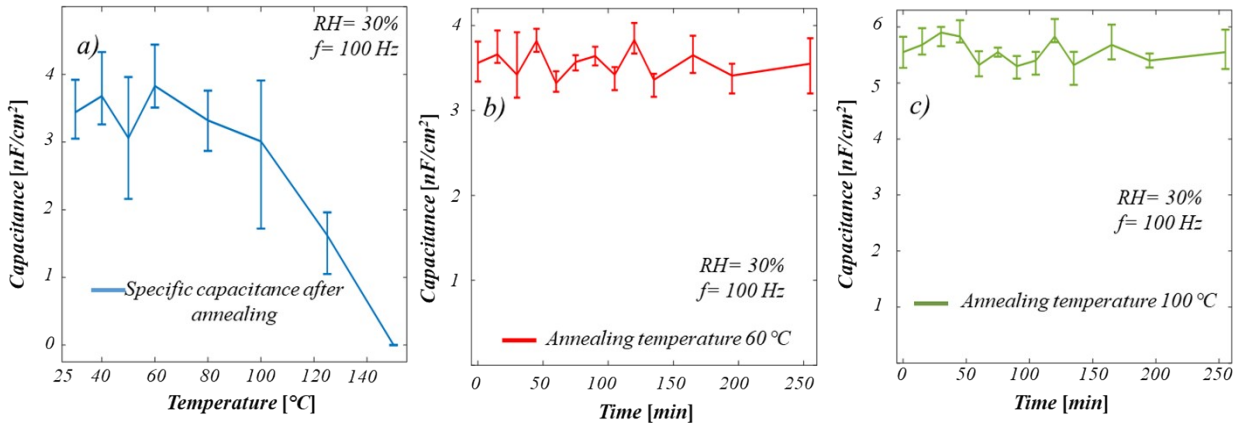

Figure S6. The irreversible variations of the *SC* of GO/Zn samples caused by thermal annealing; (**a**)-(**c**) have the same significances as the respective frames in **Figures 2**.

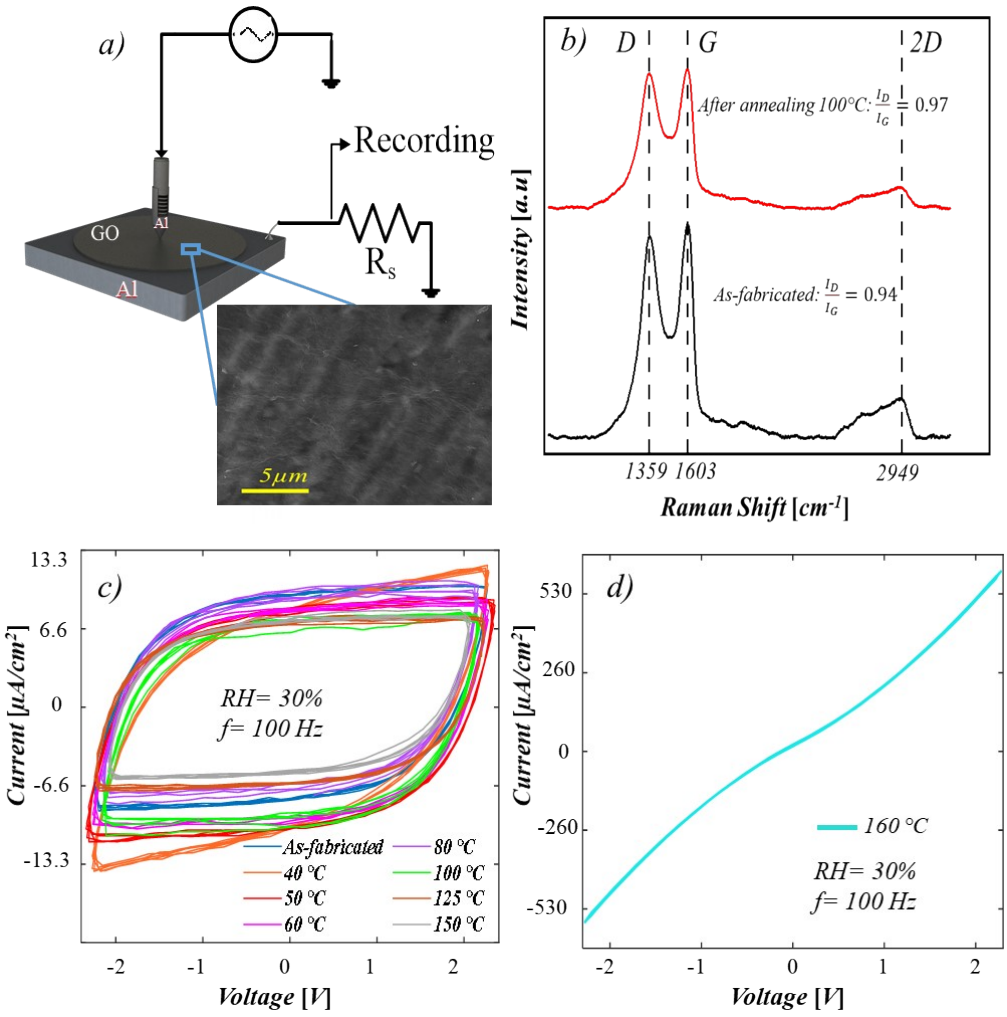

Figure S7. The characterization results on a GO/Al sample; the presented frames have the same significances as the respective ones in **Figure 1**.

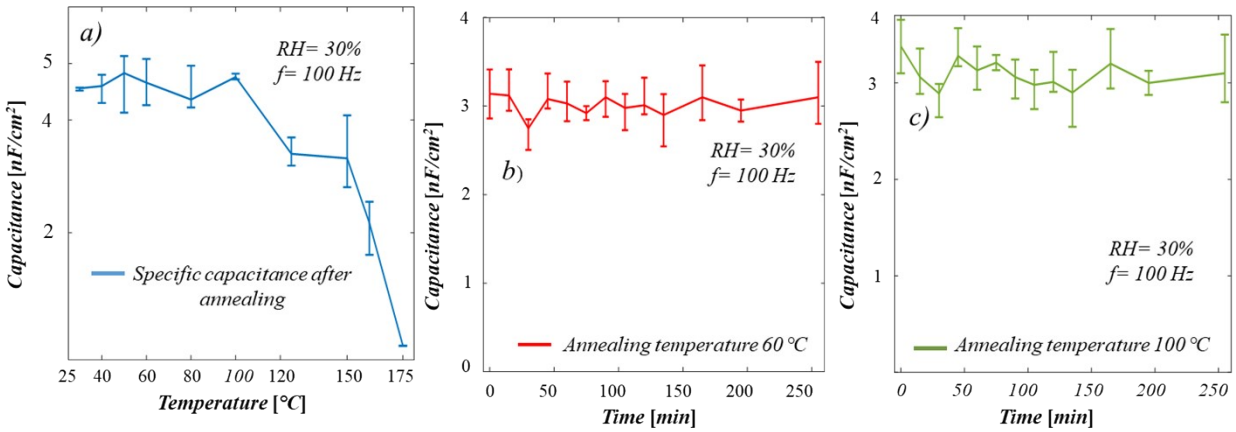

Figure S8. The irreversible variations of the *SC* of GO/Al samples caused by thermal annealing; (**a**)-(**c**) have the same significances of the respective frames in **Figures 2** for the GO/Al samples.

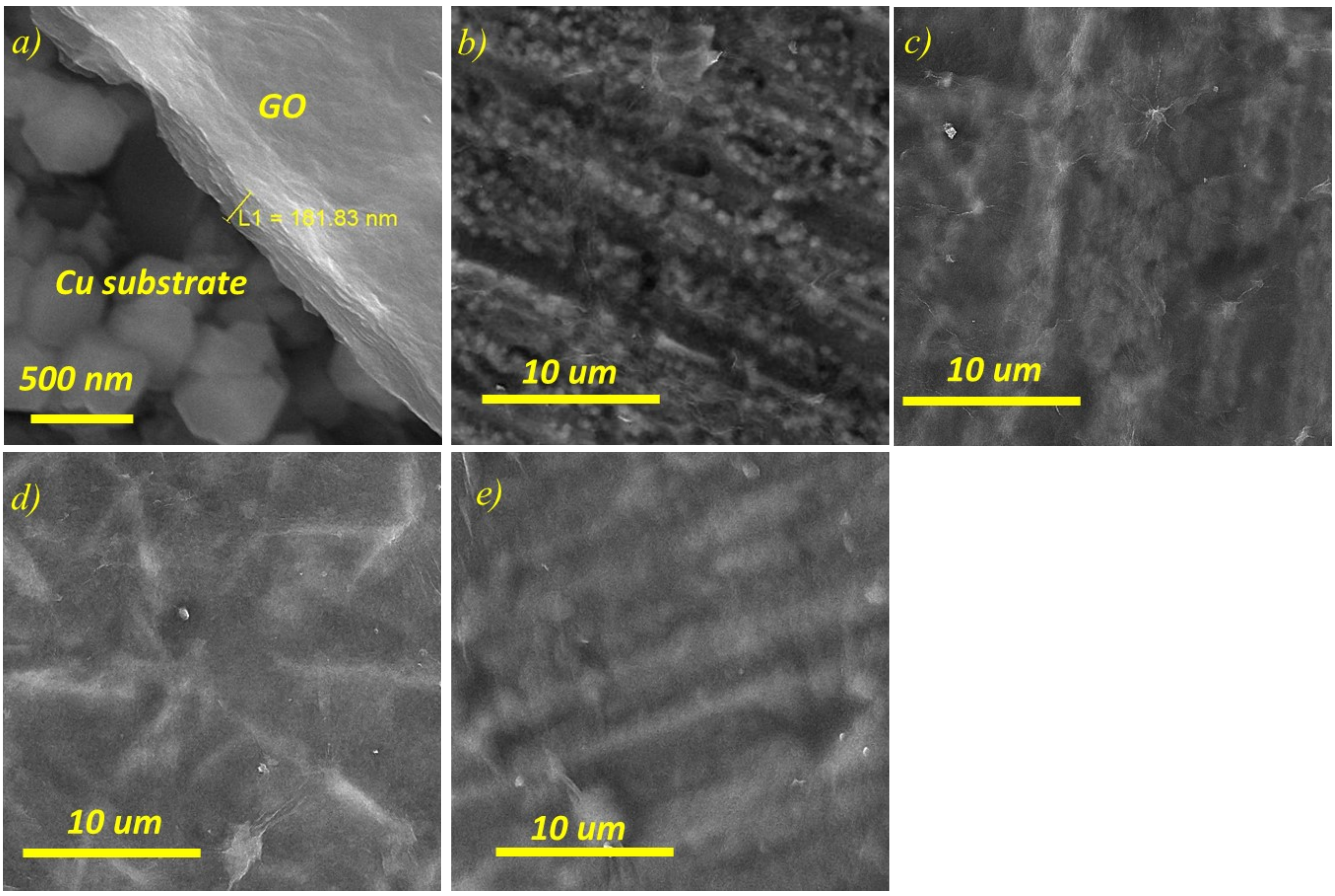

Figure S9. The plan view FESEM micorgaphes of GO on metal substrates before annealing; (a) on Cu substrate depicting a GO thickness of 180 nm**,** (b) on Cu, (c) on Al, (d) on Zn substrate, and (e) on Ti.

6. The system used for I-V plotting

The I-V characteristic recording setup comprises: a function generator for generating triangular voltage waveform with predetermined amplitude and frequency; a 2-channel oscilloscope displaying Lissajous curves of device; the interface circuits, voltage amplifiers, and buffers encompassing high precision OP177 op-amp; and a 12 bit data acquisition card with 10^5 sample/s acquisition rate converting our analogue information to digital for each channel. The latter provides conversion accuracy of +/-0.1 % of the full scale in voltage and +/-10 μs in time. Data recording and processing unit operates in the Simulink environments of MATLAB. For mitigating the error levels, the offset of each op-amp is nulled with biasing using a calibrator. A voltage buffer circuit is used before amplifier to overcome the effect of loading. For calibration of system, open and short circuit tests are carried out to determine the real offset values of voltage and current caused by the noise or circuit parameters' drifts. Also, standard resistors and capacitors are tested for final calibrations before tests. Using a triangular voltage waveform at 100 Hz, test time is 0.05 s which is includes 5 cycles of sweeping; the sampling rate is 50000 sample/s, which is 50 times larger than the signal frequency. All I-V plots presented in the manuscript are for 5 cycles showing almost no sign of parameter drift. A single measurement provide 2500 voltage-current data. A "moving average low pass filter" is used for recovering the signals buried in noise. The slew rate of the op-amps is 0.3 V/μs which is higher than the voltage scan rate (400 V/s). Therefore, the signal shapes are not affected by the circuit, and the signals related to current and voltage are read by card simultaneously. Typically, the amplitude of the applied voltage signal is $4V_{pp}$, which is read by data acquisition card after passing through a layer of voltage buffer. For current measurements, the voltage signal dropped on a series resistor is read via another voltage buffer and a non-inverting voltage amplifier. The readout is divide by the nominal value of the series resistor and the overall amplification gain. To ensure precision in the cases of high impedance samples (e.g. GO/Cu) series resistances as high as 100 kΩ are used. Then, adjusting the amplification gain at 101, the error level in the current measurement would be +/- 0.1 nA. [31, 78,104-106]

References:

S1. Y. Hu, H. Cheng, F. Zhao, N. Chen, L. Jiang, Z. Feng and L. Qu, *Nanoscale*, 2014, 6, 6448-6451.

S2. C. Ogata, R. Kurogi, K. Hatakeyama, T. Taniguchi, M. Koinuma and Y. Matsumoto, *Chemical Communications*, 2016, **52**, 3919-3922.

S3. C. Ogata, R. Kurogi, K. Awaya, K. Hatakeyama, T. Taniguchi, M. Koinuma and Y. Matsumoto, *ACS Applied Materials & Interfaces*, 2017, **9**, 26151-26160.

S4. W. Gao, N. Singh, L. Song, Z. Liu, A. L. M. Reddy, L. Ci, R. Vajtai, Q. Zhang, B. Wei and P. M. Ajayan, *Nature Nanotechnology*, 2011, **6**, 496-500.

S5. Z. Liu, Y. Dong, X. Qi, R. Wang, Z. Zhu, C. Yan, X. Jiao, S. Li, L. Qie, J. Li and Y. Huang, Energy & Environmental Science, 2022, 15, 5313-5323.

S6. Z. Yao, Q. Wu, K. Chen, J. Liu and C. Li, Energy & Environmental Science, 2020, 13, 3149-3163.